EURASIAN PHYSICAL TECHNICAL JOURNAL
2025, Volume 22, No. 2 (52)
https://doi.org/10.31489/2025N2/5-12

Received: 26/02/2025 Revised: 11/06/2025 Accepted: 23/06/2025

Research Article

UDC 535.015, 535.2, 538.975

THE EFFECT OF THE INTERNAL HEAVY ATOM ON SINGLET OXYGEN GENERATION IN THE PRESENCE OF PLASMONIC NANOPARTICLES

Ibrayev N.Kh.*, Menshova E.P.

Institute of Molecular Nanophotonics, Buketov University, Karaganda, Kazakhstan
*Corresponding author: niazibrayev@mail.ru

Abstract. *The heavy atom effect on singlet oxygen generation in the plasmon field of silver nanoparticles was investigated. The dyes rhodamine 123 and dibromrhodamine 123 in polyvinyl butyral films were used as sensibilisers. The dye films were deposited by spin-coating onto silver island films synthesised on the quartz surface. The results showed that the presence of bromine atom in the dye molecules increased the singlet oxygen generation efficiency. The calculated Stern-Follmer constants demonstrate the enhancement of molecular oxygen quenching of triplet states of dibromorhodamine 123 dye molecules in the presence of Ag nanoparticles.*

Keywords: heavy atom effect, intersystem crossing, singlet oxygen, nanoplasmonics, photosensitiser.

1. Introduction

Singlet oxygen $O_2(^1\Delta_g)$ is the most stable excited state of molecular oxygen $O_2(^3\Sigma_g)$ which plays an important role in biological, chemical and industrial processes, acting as the main oxidant. It is highly sought after for photodynamic therapy, which is used in the therapeutic and/or palliative treatment of various cancers and benign diseases. The mechanism of cell destruction underlying photodynamic therapy combines the activation of sensitising molecules by light irradiation and the formation of singlet oxygen and cytotoxic reactive oxygen species (ROS). In addition, $O_2(^1\Delta_g)$ and ROS can act as oxidants in biological objects [1,2] and in organic synthesis [3,4], be used for light inactivation of proteins using chromophores [5] and photodegradation of organic contaminants [5,6], disinfection of drinking water [7], sterilisation of gases and solids, and self-cleaning of filter membranes [8].

To study the processes of molecular oxygen $O_2(^3\Sigma_g^-)$ activation, photosensitizers (PSs) based on organic dyes with high quantum yield to the triplet state and the ability to transfer energy to $O_2(^3\Sigma_g^-)$ oxygen are used [9]. One of the factors that increase the probability of intersystem crossing (ISC) and, consequently, the transition of sensitising molecules to the triplet state [10], is the adding of heavy atoms to the structure of dye molecules. This approach found wide application in the development of new PSs for photodynamic therapy and other fields requiring efficient generation of reactive oxygen species [11].

Much attention is also paid to the study of the interaction of organic photosensitisers with plasmonic nanoparticles (NPs), which can significantly enhance the luminescence intensity and shorten the phosphorescence lifetime due to the Purcell effect [12]. In the presence of silver or gold NPs, the local electromagnetic field is enhanced, that increases the probability of radiative transitions and accelerates the deactivation of excited states of the sensitiser [13]. Plasmon NPs can also increase the sensitivity and selectivity of sensitisers to oxygen due to more efficient energy transfer from the triplet state of the sensitiser to the oxygen molecule [14]. In particular, the use of silver island films (SIFs) allows achieving enhanced luminescence due to the generation of localised surface plasmons and increasing the overall signal intensity [15]. In [16,17] a correlation between the effect of the heavy atom in the dye molecule and the degree of influence of the plasmon effect of silver NPs on the phosphorescence properties of a series of halogen-substituted xanthene and fluorescein dyes was carried out. A theoretical model is proposed to estimate the quantum yield of phosphorescence of dye molecules in the vicinity of plasmonic NPs. To this end, the rate constants of radiative and non-radiative intramolecular transitions of dyes were calculated.

This study is an extension of [16] using brominated rhodamine derivatives and silver plasmonic structures to improve the efficiency of singlet oxygen generation. The use of heavy atoms together with plasmonic NPs opens up the prospect of creating more efficient and precise photosensitisers for the targeted generation of reactive oxygen species [18].

2. Experimental part

The dyes rhodamine 123 (Rh123) and dibromhodamine 123 (Rh 123-2Br), which were purchased from Sigma-Aldrich, were chosen to study the effect of spin-orbit interaction on $O_2(^1\Delta_g)$ generation. The molecular structure of the dye molecules studied is shown in Figure 1. The dye films in polyvinyl butyral (PVB) were deposited by spin-coating at 1,500 rpm for 30 sec. The concentration of dyes in 7 wt% polymer was $5 \cdot 10^{-4}$ mol/L. Micro-weighing was used to control the thickness of films deposited on different substrates. The mass of the dye films on the surface was almost the same. The oxygen permeability of PVB is 0.95×10^{-10} $cm^3 \cdot cm/(cm^2 \cdot s \cdot atm)$ [19].

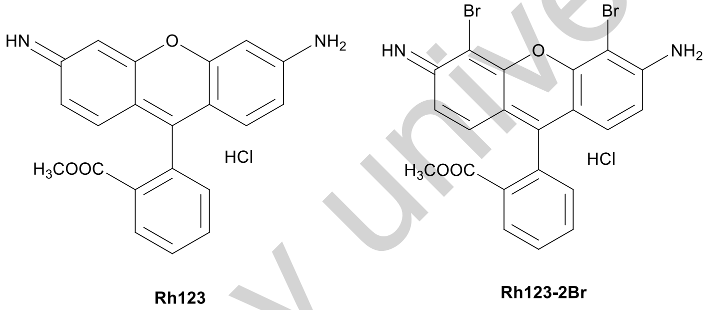

Fig. 1. Molecular structure of the investigated dye molecules

To study the effect of plasmonic NPs on $O_2(^1\Delta_g)$ generation in the presence of heavy atom, substrates of SIFs were prepared by chemical deposition [20]. Analytical grade purity chemicals from Sigma Aldrich and ultrapure water obtained using a Smart S15 UVF system (Drawell) were used to SIFs synthesise. SIFs were annealed at 240^{0}C for 30 min. This in turn helps to stabilise and improve the structural and functional properties of the silver films. According to scanning electron microscope (Mira 3LMU, Tescan) data, spherical islands of size 105 – 375 nm were uniformly distributed on the film's surface of the (Fig. 2a).

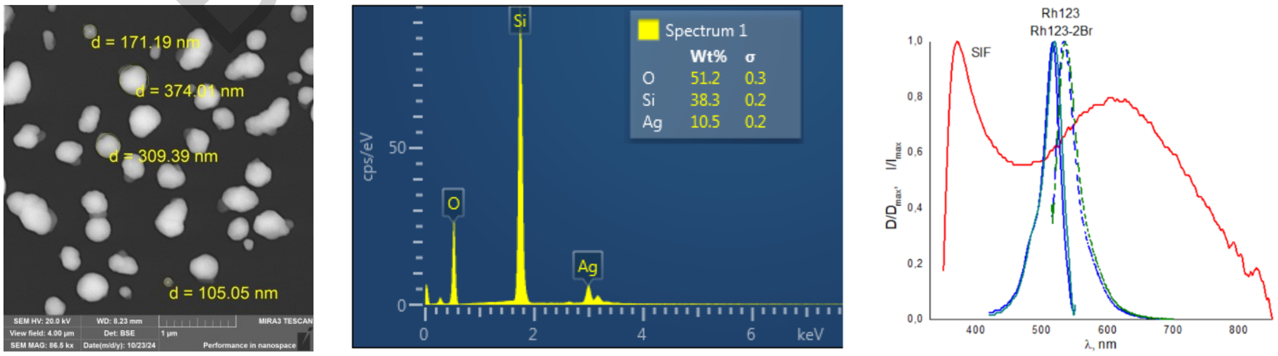

Spectrum 1

	Wt%	σ
O	51.2	0.3
Si	38.3	0.2
Ag	10.5	0.2

a b c

Fig. 2. (a) SEM image of SIFs obtained by chemical deposition on quartz glass, (b) XPS spectra of SIFs and (c) Absorption spectra of SIFs (red line), Rh123 (blue solid), Rh123-2Br (green solid) and fluorescence spectra of Rh123 (blue dashed), Rh123-2Br (green dashed) in PVB film on quartz glass ($\lambda_{exc} = 510$ nm, $\lambda_{reg} = 540$ nm)

Energy dispersive X-ray spectroscopy analysis of the SIFs surface showed the presence of silver, silicon and oxygen, where silicon and oxygen are related to the composition of quartz glass (Fig. 2b). The absorption spectrum of SIFs is broadened and has two peaks at 365 nm and 605 nm (Fig. 2c). The broadening is due to the large variation in the size of the islands.

Cary 300 and Eclipse spectrometers (Agilent Technologies) were used to record absorption, fast and delayed fluorescence spectra. Delayed fluorescence (DF) and phosphorescence (Phos) measurements of Rh123 and Rh123-2Br films were carried out under varying pressure conditions using an Optistat DN vacuum cryostat (Oxford Instruments).

A FLS1000 spectrometer (Edinburgh Instruments) with UV, Vis-PMT and NIR-PMT photomultipliers (Hamamatsu) was used to record the attenuation kinetics of long-lived luminescence of dyes and singlet oxygen phosphorescence. Photoexcitation of samples at λ_{exc}=510 nm was carried out by a laser system based on Nd:YAG laser LQ529 with OPO LP604 and second harmonic generator LG305 (SolarLS).

3. Results and Discussion

From the normalised absorption and fluorescence spectra of Rh123 and Rh123-2Br in the polymer films, it can be seen that the spectra of Rh123-2Br are bathochromically shifted, due to the presence of two bromine atoms (Fig. 2c). The maximum of the absorption spectrum (λ_{abs}^{max}) of Rh123 falls at 516 nm, Rh123-2Br – at 520 nm. The maximum of fluorescence spectrum (λ_{fl}^{max}) is at 535 nm for Rh123 and at 540 nm for Rh123-2Br. Figure 3 shows the long-lived luminescence spectra of the dye films, where two luminescence maxima are expressed. The first maximum at 540 nm coincides with the fast fluorescence and refers to DF. Whereas the maximum at around 670 nm is Phos of the dyes (Fig. 3).

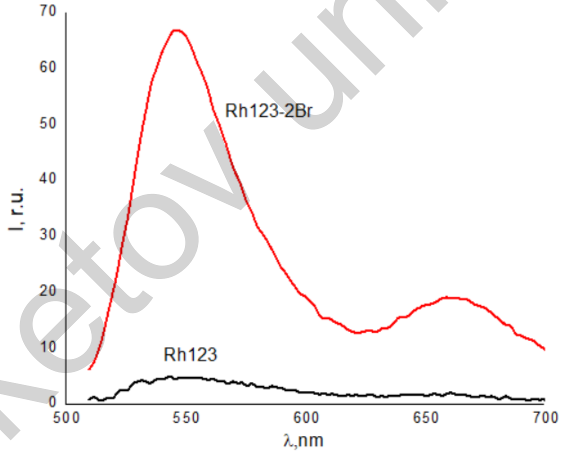

Fig. 3. Long-lived luminescence spectra of Rh123 and Rh123-2Br (5*10^{-4} mol/L) in PVB film (7 wt%) (λ_{exc} = 510 nm) at cryostat air pressure of 10^{-3} mB and T = 293 K

From the I_{DF}/I_{Phos}, intensities ratio, which is 2.5 for the first dye and 3.2 for the second dye, it can be stated that Rh123-2Br has more pronounced phosphorescence than Rh123. DF and Phos intensities of the Br-substituted dye are an order of magnitude higher than those of Rh123. The shorter lifetime of DF and Phos of Rh123-2Br (Table 1) is due to the faster decay of the S_1 state not only to the ground state, but also to the nearby triplet state T_1 due to the increase in the probability of ISC due to the effect of the internal heavy atom [17].

The effect of oxygen concentration on the DF and Phos of Rh123-2Br was studied (Fig. 4). Dibromorhodamine molecules have a high probability of transition from the excited singlet state (S_1) в to the triplet state (T_1) due to ISC, which is characteristic of molecules containing heavy atoms.

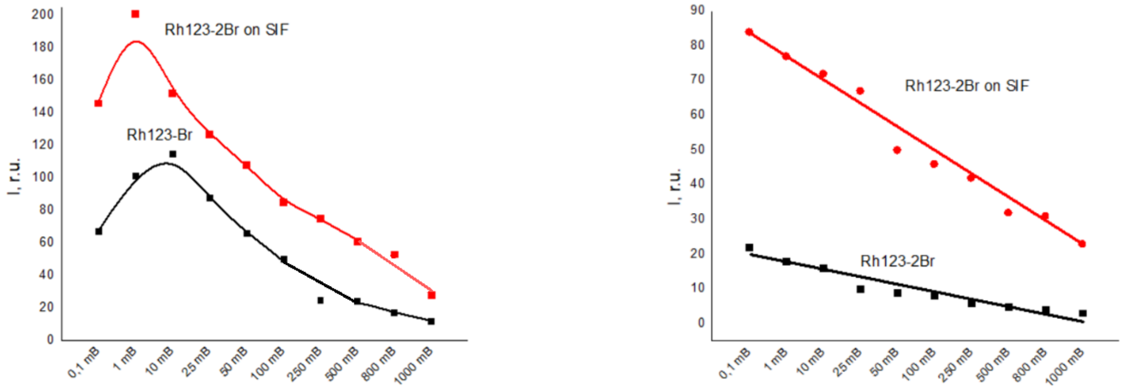

a b

Fig. 4. The dependence of the intensity of DF (a) and Phos (b) of Rh123-2Br in PVB films on the cryostat pressure (λ_{exc} = 510 nm, λ_{reg} = 540 nm for DF and λ_{reg} = 670 nm for Phos) at T = 293K

According to [21], the following processes can occur in the collision complexes of molecular oxygen and triplets of the sensitiser:

$$T + {}^3\Sigma_g^- \rightarrow \left[T\mathrm{K}\,{}^3\Sigma_g^-\right]^{1,3,5} \rightarrow S_0 + {}^1\Delta_g \quad (1)$$

$$T + {}^1\Delta_g \rightarrow \left[T\mathrm{K}\,{}^1\Delta_g\right]^3 \rightarrow S_1 + {}^3\Sigma_g^- \rightarrow S_0 + {}^3\Sigma_g^- + h\nu_{DF} \quad (2)$$

$${}^1\Delta_g \rightarrow {}^3\Sigma_g^- + h\nu_{Phos} \quad (3)$$

where S_0, S_1, T – ground, excited singlet and triplet states, ${}^3\Sigma_g^-$, ${}^1\Delta_g$ – molecular and singlet oxygen, $\left[T\mathrm{K}\,{}^3\Sigma_g^-\right]^{1,3,5}$ – intermediate complex between the sensitiser and oxygen, where the total spin multiplicity can be 1 (singlet), 3 (triplet), or 5 (quintet), $\left[T\mathrm{K}\,{}^1\Delta_g\right]^3$ – excited complex of the sensitiser with singlet oxygen, forming a triplet state, $h\nu_{DF}$ – photon emitted as DF of sensitiser, $h\nu_{Phos}$ – photon emitted during phosphorescence of singlet oxygen.

Process 1 is singlet oxygen sensitisation reaction; process 2 – singlet-triplet annihilation reaction; process 3 – generation of singlet oxygen phosphorescence.

Under the influence of an enhanced plasmon field, the intensity of all types of luminescence increases, as the probability of transition between energy levels increases and more dye molecules return to the ground state with the emission of light photons [22]. The intensity of fast fluorescence increased 2.6 times for Rh123 and 2.18 times for Rh123-2Br. Also, in the presence of plasmon, there is an increase in DF intensity by 2.4 and 2.18 times and Phos intensity by 3.5 and 3.81 times for Rh123 and Rh123-2Br, respectively (Table 1). While the luminescence lifetime decreases (Table 1).

This phenomenon is described by the Purcell effect, according to which near metallic nanostructures possessing plasmons, the lifetime of excited states decreases as rates of radiative transitions are amplified due to the local plasmon field. As a result, the long-lived luminescence becomes more intense, but its lifetime decreases [14, 23, 24].

Figure 4 shows the dependences of the intensity of DF and Phos of Br-substituted dye without the influence of plasmons and in its presence on the air pressure in the cryostat. For DF (Fig. 4a) on quartz glass and on SIFs, an increase of the luminescence intensity with pressure changes from 0.1 to 10 mB, and then a decrease is observed, that is a confirmation of singlet-triplet annihilation. While the Phos intensity (Fig. 4b) decreases monotonically. It is worth noting that the deactivation process of triplet states is more pronounced for Rh123-2Br in the presence of plasmon. The Phos quenching constants by oxygen molecules were calculated on the basis of the Stern-Folmer equation [25]:

$$\frac{I_{Phos}^{0}}{I_{Phos}} = 1 + k_q \tau_0 \cdot [Q], \qquad (4)$$

where I_{Phos}^{0} – Phos intensity in the absence of O_2, I_{Phos} – Phos intensity in the presence of O_2, k_q – extinction coefficient, τ_0 – Phos lifetime in the absence of O_2, a $[Q]$ – O_2 concentration.

Table 1. Spectral-luminescence parameters of Rh123 and Rh123-2Br in PVB films

	λ^{max}_{abs} (nm)	D	λ^{max}_{fl} (nm)	I_{fl} (r.u.)	I_{DF} (r.u.)	τ_{DF} (ms)	I_{Phos} (r.u.)	τ_{Phos} (ms)	D/D_0	$I_{fl}/I_{fl\,0}$	$I_{DF}/I_{DF\,0}$	$\tau_{DF}/\tau_{DF\,0}$	I_{Phos}/I_{Phos0}	τ_{Phos}/τ_{Phos0}
						Rh123								
Quartz	516	0.12	535	163	5	8.7±0.2	2	7.4±0.3	-	-	-	-	-	-
SIFs		0.16		423	12	8.5±0.1	7	5.7±0.7	1.33	2.60	2.4	0.97	3.5	0.77
						Rh123-2Br								
Quartz	520	0.13	540	93	67	5.0±0.4	22	5.9±0.1	-	-	-		-	
SIFs		0.15		204	146	4.8±0.2	84	3.6±0.2	1.13	2.18	2.18	0.96	3.81	0.61

Figure 5 shows that a stronger quenching of the triplet state of the dye by oxygen molecules is observed in the plasmon field. For Rh123-2 films on glass k_q =6,2 • 10^2 $M^{-1}s^{-1}$, and on Ag island films k_q =9,1 • 10^2 $M^{-1}s^{-1}$.

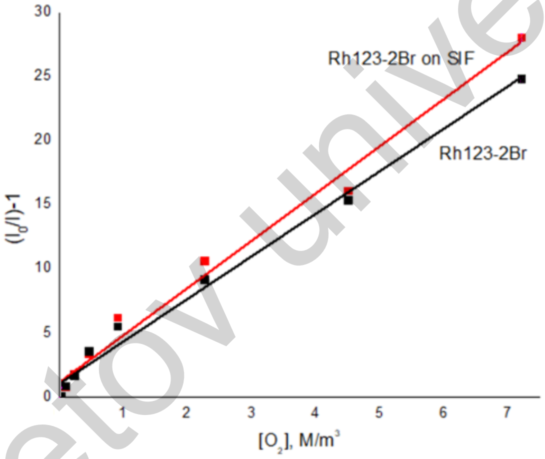

Fig. 5. Stern-Follmer quenching constants of R123-2Br phosphorescence by O_2 molecules on quartz (red line) and on SIFs (black line)

The value of the quenching constant (k_q) can be used as an indicator of the efficiency of singlet oxygen generation. Since k_q reflects how efficiently oxygen quenches the triplet state of the dye-sensitiser. Its value can be indirectly related to the singlet oxygen yield. The higher k_q, the more triplet states of the sensitiser transfer their energy to oxygen molecules as a result of heteroannihilation, that leads to an increase in the singlet oxygen yield $^1\Delta_g$.

Upon photoexcitation, phosphorescence of singlet oxygen was observed in the absorption band of Rh123-2Br, while Rh123 does not contribute to its effective generation. Under the influence of plasmonic field of SIFs the singlet oxygen generation sensitised by Rh123-2Br increased by 2.49 times (Fig. 6).

The kinetic of singlet oxygen phosphorescence is represented by two phases: rise and decay (Fig. 6) and can be approximated according to a two-exponential equation:

$$I(t) = I_0 \left[\exp\left(-\frac{t}{\tau_{decay}} \right) - \exp\left(-\frac{t}{\tau_{rise}} \right) \right] \qquad (5)$$

where $I(t)$ – phosphorescence intensity of $O_2(^1\Delta_g)$ per second, I_0 – pre-exponential multiplier, τ_{decay} and τ_{rise} – time constants of the decay and rise phases [26].

The rise phase is determined by the rate of singlet oxygen formation as a result of energy transfer from the triplets of Rh123-2Br to $O_2(^3\Sigma_g^-)$, the decay phase – by the process of singlet oxygen deactivation.

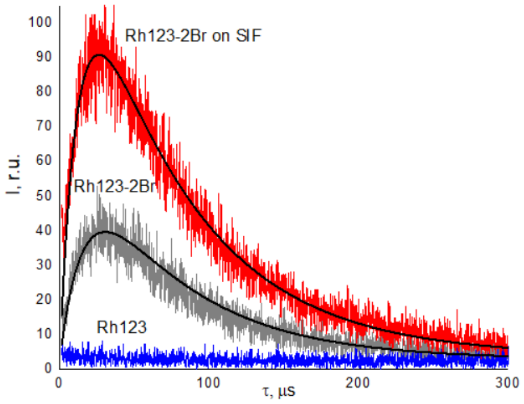

Fig. 6. Kinetics of singlet oxygen phosphorescence (λ_{reg} = 1270 nm) sensitised by R123 and R123-2Br dyes on quartz and SIFs at atmospheric pressure (λ_{exc} = 510 nm)

According to the fitting results, the duration of the rising phase was 16.13 μs and the duration of the decay phase was 75.60 μs. Under the action of plasmon, the duration of these phases decreased by 14% and 3%, respectively. (Table 2). The decrease of the lifetime of $O_2(^1\Delta_g)$ phosphorescence is associated with the enhancement of the radiation transition $^1\Delta_g \rightarrow {}^3\Sigma_g^-$.

Table 2. Plasmon effects on the intensity and lifetime of singlet oxygen phosphorescence (λ_{reg} = 1270 nm at atmospheric pressure (λ_{exc} = 510 nm)

	I, r.u.	τ_{rise}, μs	τ_{decay}, μs	I/I_0	$\tau_{rise}/\tau_{rise\ 0}$	$\tau_{decay}/\tau_{decay\ 0}$
$O_2(^1\Delta_g)$ on quartz	60	16.13±0.77	75.60±0.91	-	-	-
$O_2(^1\Delta_g)$ on SIFs	112	12.25±1.61	71.89±0.61	2.49	0.76	0.95

4. Conclusions

In this study, a comparative analysis of the singlet oxygen $O_2(^1\Delta_g)$ generation efficiency by Rh123 and Rh123-2Br dyes in polymer films in the presence of plasmonic silver NPs was carried out. The addition of a heavy bromine atom into Rh 123 molecules leads to a significant increase of the probability of ISC and singlet oxygen generation, as evidenced by an increase of the intensity and decrease in the phosphorescence lifetime. The presence of silver plasmonic NPs further enhances the luminescence processes due to the Purcell effect, reducing the lifetime of excited states and increasing the luminescence intensity. The Stern-Volmer constants for Rh123-2Br on SIFs substrates show a higher quenching coefficient, indicating an increase of the energy transfer efficiency of oxygen molecules and singlet oxygen generation in the plasmon field.

Conflict of interest statement

The authors declare that they have no conflict of interest in relation to this research, whether financial, personal, authorship or otherwise, that could affect the research and its results presented in this paper.

CRediT author statement

Ibrayev N.Kh.: supervision, resources, conceptualization, validation; **Menshova E.P.**: formal analysis, investigation writing - original draft, visualization. All authors have read and agreed to the published version of the manuscript.

Acknowledgements

This research is funded by the Science Committee of the Ministry of Science and Higher Education of the Republic of Kazakhstan (Grant No. AP23490195).)

References

1 Sagadevan A., Hwang K.C., Su M.D. (2017) Singlet oxygen-mediated selective C–H bond hydroperoxidation of ethereal hydrocarbons. *Nature Communications*, 8(1), 1812. https://doi.org/10.1038/s41467-017-01906-5

2 Schmidt R. (2006). Photosensitized generation of singlet oxygen. *Photochemistry and Photobiology*, 82(5), 1161–1177. https://doi.org/10.1562/2006-03-03-IR-833

3 Ishchenko A.A., Syniugina A.T. (2023) Structure and photosensitiser ability of polymethine dyes in photodynamic therapy: *A review. Theoretical and Experimental Chemistry*, 58(6), 373–401. https://doi.org/10.1007/s11237-023-09754-9

4 Singleton D. A., Hang C., Szymanski M. J., Meyer M. P., Leach A. G., Kuwata K. T., Chen J. S., Greer A., Foote C.S., Houk K.N. (2003) Mechanism of the reactions of singlet oxygen: A two-step no-intermediate mechanism. *Journal of the American Chemical Society,* 125(5), 1319–1328. https://doi.org/10.1021/ja027225p

5 Aerssens D., Cadoni E., Tack L., Madder A. (2022) A photosensitized singlet oxygen (1O2) toolbox for bio-organic applications: Tailoring $^1O_2$ generation for DNA and protein labelling, targeting and biosensing. *Molecules*, 27(3), 778. https://doi.org/10.3390/molecules27030778

6 Bregnhøj M., Prete M., Turkovic V., Petersen A. U., Nielsen M.B., Madsen M., Ogilby P.R. (2019) Oxygen-dependent photophysics and photochemistry of prototypical compounds for organic photovoltaics: Inhibiting degradation initiated by singlet oxygen at a molecular level. *Methods and Applications in Fluorescence*, 8(1), 014001. https://doi.org/10.1088/2050-6120/ab4edc

7 Pibiri I., Buscemi S., Palumbo Piccionello A., Pace A. (2018) Photochemically produced singlet oxygen: Applications and perspectives. *ChemPhotoChem*, 2(7), 535–547. https://doi.org/10.1002/cptc.201800076

8 Wang Y., Lin Y., He S., Wu S., Yang C. (2024). Singlet oxygen: Properties, generation, detection, and environmental applications. *Journal of Hazardous Materials,* 461, 132538. https://doi.org/10.1016/j.jhazmat.2023.132538

9 Khan A., Alam M., Rehman S. U., Khan G. S., Khan F.A., Khan M., Zhang Y. (2019) Rhodamine-based fluorescent probes for bioimaging applications. *Chemical Reviews*, 119(19), 10504–10555. https://doi.org/10.1021/acs.chemrev.9b00230

10 Rao D., Singh P., Jain R. (2020) Applications of singlet oxygen in photodynamic therapy enhanced by plasmonic nanostructures. *Journal of Biomedical Nanotechnology,* 16(5), 843–856. https://doi.org/10.1166/jbn.2020.2914

11 Ogawa K., Kobuke Y. (2016) Heavy atom effects in photochemical and photobiological applications. *Accounts of Chemical Research*, 49(5), 712–721. https://doi.org/10.1021/acs.accounts.6b00027

12 Lakowicz J.R. (2006) Principles of fluorescence spectroscopy (3rd ed.). Springer. https://doi.org/10.1007/978-0-387-46312-4

13 Chowdhury M.H., Ray K. (2008) Plasmon-controlled fluorescence towards high-sensitivity optical sensing. *Advances in Biochemical Engineering/Biotechnology*, 116, 29–72. https://doi.org/10.1007/10_2008_9

14 Ray K., Chowdhury M.H., Zhang J., Fu Y., Szmacinski H., Nowaczyk K., Lakowicz J.R. (2009) Plasmon-controlled fluorescence towards high-sensitivity optical sensing. *Advances in Biochemical Engineering/Biotechnology*, 116, 29–72. https://doi.org/10.1007/10_2008_9

15 Zhang Y., Xu C., Hao Y. (2015) Influence of heavy atoms on intersystem crossing and singlet oxygen generation in photodynamic systems. *Journal of Photochemistry and Photobiology A: Chemistry*, 306, 44–52. https://doi.org/10.1016/j.jphotochem.2015.04.006

16 Ibrayev N.K., Valiev R.R., Seliverstova E.V., Menshova E.P., Nasibullin R.T., Sundholm D. (2024) Molecular phosphorescence enhancement by the plasmon field of metal nanoparticles. *Physical Chemistry Chemical Physics*, *26*(20), 14624–14636. https://doi.org/10.1039/d4cp01281j

17 Ibrayev N., Seliverstova E., Valiev R., Aymagambetova A., Sundholm D. (2024). The effect of heavy atoms on the *deactivation of electronic excited states of dye molecules near the surface of metal nanoparticles. Physical Chemistry Chemical Physics,* 26(40), 25986–25993. https://doi.org/10.1039/D4CP02621G

18 DeRosa M.C., Crutchley R.J. (2002). Photosensitized singlet oxygen and its applications. *Coordination Chemistry Reviews,* 233–234, 351–371. https://doi.org/10.1016/S0010-8545(02)00034-6

19 Kamalova D.I., Abdrazakova L.R., Salakhov M.Kh. (2020) Poly(vinyl butyral)/poly(ethylene glycol) blends for gas separation membranes: Coefficients of diffusion and permeability of oxygen. *Journal of Non-Crystalline Solids*, 532, 120304. https://doi.org/10.1016/j.jnoncrysol.2020.120304

20 Ibrayev N., Seliverstova E., Temirbayeva D., Ishchenko A. (2022) Plasmon effect on simultaneous singlet-singlet and triplet-singlet energy transfer. *Journal of Luminescence,* 251, 119203. https://doi.org/10.1016/j.jlumin.2022.119203

21 Minaev B.F. (2007) Electronic mechanisms of molecular oxygen activation. *Russian Chemical Reviews*, 76(11), 988–1010. https://doi.org/10.1070/RC2007v076n11ABEH003720

22 Seliverstova E., Ibrayev N., Omarova G., Ishchenko A., Kucherenko M. (2021) Competitive influence of the plasmon effect and energy transfer between chromophores and Ag nanoparticles on the fluorescent properties of indopolycarbocyanine dyes. *Journal of Luminescence*, 235, 118000. https://doi.org/10.1016/j.jlumin.2021.118000

23 Kanapina A., Seliverstova E., Ibrayev N., Derevyanko N., Ishchenko A. (2023) Features of the decay of excited states of ionic dyes in the near field of metal nanoparticles. *Eurasian Physical Technical Journal,* 20, 2(44), 106–111. https://doi.org/10.31489/2023No2/106-111

24 Temirbayeva D., Ibrayev N., Kucherenko M. (2022). Distance dependence of plasmon-enhanced fluorescence and delayed luminescence of molecular planar nanostructures. *Journal of Luminescence*, 243, 118642. https://doi.org/10.1016/j.jlumin.2021.118642

25 Gehlen M. H. (2020) The centenary of the Stern–Volmer equation of fluorescence quenching: From the single line plot to the SV quenching map. *Journal of Photochemistry and Photobiology C: Photochemistry Reviews,* 42, 100338. https://doi.org/10.1016/j.jphotochemrev.2019.100338

26 Krasnovsky A.A. (2008) Luminescence and photochemical studies of singlet oxygen photonics. *Journal of Photochemistry and Photobiology A: Chemistry*, 196(2–3), 210–218. https://doi.org/10.1016/j.jphotochem.2007.12.015

AUTHORS' INFORMATION

Ibrayev, Niyazbek – Doctor of Physics and Mathematical Sciences, Professor, Professor-researcher, Director of the Institute of Molecular Nanophotonics, Buketov Karaganda University, Karaganda, Kazakhstan; SCOPUS Author ID: 9333698600, https://orcid.org/0000-0002-5156-5015; niazibrayev@mail.ru.

Menshova, Evgeniya – Master (Eng.), Junior Research Fellow, Institute of Molecular Nanophotonics, Buketov Karaganda University, Karaganda, Kazakhstan; SCOPUS Author ID: 57283853000, https://orcid.org/0000-0003-3646-3763; menshovayevgeniya@gmail.com